Far-infrared conductivity in electron-doped cuprate $La_{2-x}Ce_xCuO_4$

A. Pimenov[1], A. V. Pronin[1,2], A. Loidl[1], A. Tsukada[3] and M. Naito[3]

[1] *Experimentalphysik V, EKM, Universität Augsburg - 86135 Augsburg, Germany*
[2] *General Physics Institute of the Russian Academy of Sciences 119991 Moscow, Russia*
[3] *NTT Basic Research Laboratories - 3-1, Morinosato-Wakamiya Atsugi-shi, Kanagawa 243-0198, Japan*

Abstract. – We performed far-infrared and submillimeter-wave conductivity experiments in the electron-doped cuprate $La_{2-x}Ce_xCuO_4$ with $x = 0.081$ (underdoped regime, $T_c = 25\,K$). The onset of the absorption in the superconducting state is gradual in frequency and is inconsistent with the isotropic *s*-wave gap. Instead, a narrow quasiparticle peak is observed at zero frequency and a second peak at finite frequencies, clear fingerprints of the conductivity in a *d*-wave superconductor. A far-infrared conductivity peak can be attributed to $4\Delta_0$, or to $2\Delta_0 + \Delta_{spin}$, where Δ_{spin} is the resonance frequency of the spin fluctuations. The infrared conductivity as well as the suppression of the quasiparticle scattering rate below T_c are qualitatively similar to the results in the hole-doped cuprates.

Introduction. – The interest in the physical properties of electron-doped superconductors [1] has revived recently concerning the symmetry of the superconducting order parameter. Earlier results in these compounds on penetration depth [2], Raman [3] and tunneling spectroscopies [4] were explained in terms of conventional (*s*-wave) symmetry of the superconducting order parameter. However, later experiments, including half-flux effect [5], penetration-depth measurements [6], and photoemission [7], provided strong evidences for *d*-wave–type symmetry. This contradiction can possibly be resolved on the basis of recent microwave experiments [8] and point-contact spectroscopy [9], which suggest changes of the gap symmetry as a function of doping.

Electron doping of the high-T_c cuprates can be achieved by substituting Ce^{4+} into Ln_2CuO_4 with Ln = Pr, Nd, Sm, and Eu [1, 10]. Among these family $Nd_{2-x}Ce_xCuO_4$ is the earliest known and best studied compound [11]. The highest transition temperatures for electron-doped cuprates ($T_c = 30\,K$) can be achieved in $La_{2-x}Ce_xCuO_4$ (LCCO) [10]. The temperature of the superconducting transition in LCCO is close to $T_c = 39\,K$ in a recently discovered superconductor MgB_2 [12], which is believed to be of BCS type [13, 14]. In order to obtain valuable

information about the gap symmetry in LCCO, a direct comparison of the physical properties of these compounds can be carried out. Such analysis is provided by the low-frequency electrodynamics which directly visualizes many important features of superconductors as energy gap [15, 16] or quasiparticle scattering rate [17].

In this paper we present the far-infrared and submillimeter-wave conductivity of underdoped ($x = 0.081$, $T_c = 25\,\mathrm{K}$) LCCO thin film. In order to obtain the complex conductivity above and below the superconducting gap energy, two different experimental methods have been applied using the same sample. For frequencies below $40\,\mathrm{cm}^{-1}$, the complex conductivity has been obtained by the submillimeter transmission spectroscopy. At higher frequencies the reflectance was measured using standard far-infrared techniques and the conductivity has been obtained via a Kramers-Kronig analysis of the spectra.

Experimental details. – High-quality $La_{2-x}Ce_xCuO_4$ films with $x = 0.081 \pm 0.01$ (underdoped regime) were deposited by molecular-beam epitaxy [10, 18] on transparent (001) $SrLaAlO_4$ substrates $10\times10\times0.5\,\mathrm{mm}^3$ in size. The thickness of the present film was 140 nm and the film revealed a sharp transition into the superconducting state ($\Delta T_c < 1\,\mathrm{K}$) at $T_c = 25\,\mathrm{K}$. Lower transition temperature compared to the optimal doping ($x \simeq 0.11$, $T_c = 30\,\mathrm{K}$ [10, 18]) confirms the underdoped character of the sample.

The transmission experiments for frequencies $5\,\mathrm{cm}^{-1} < \nu < 40\,\mathrm{cm}^{-1}$ were carried out in a Mach-Zehnder interferometer arrangement [19] which allows both the measurements of the transmittance and the phase shift of a film on a substrate. The properties of the blank substrate were determined in separate experiments. Utilizing the Fresnel optical formulas for the complex transmission coefficient of the substrate-film system, the absolute values of the complex conductivity $\sigma^* = \sigma_1 + i\sigma_2$ were determined directly from the measured spectra. In the frequency range $40 < \nu < 8000\,\mathrm{cm}^{-1}$, reflectance measurements were performed using Bruker IFS-113v and IFS 66v/S Fourier-transform spectrometers. In addition, the reflectance for frequencies $5 < \nu < 40\,\mathrm{cm}^{-1}$ was calculated from the complex conductivity data of the same samples, which was obtained by the submillimeter transmission. This substantially improves the quality of the subsequent Kramers-Kronig analysis of the reflectance and therefore the reliability of the data especially at low frequencies.

The reflectance of a thin metallic film on a dielectric substrate can be obtained from the Maxwell equations [20]

$$r = \frac{r_{0\mathrm{f}} + r_{\mathrm{fs}} \exp[4\pi i n_{\mathrm{f}} d/\lambda]}{1 + r_{0\mathrm{f}} r_{\mathrm{fs}} \exp[4\pi i n_{\mathrm{f}} d/\lambda]}\,, \tag{1}$$

with $r_{0\mathrm{f}} = (1-n_{\mathrm{f}})/(1+n_{\mathrm{f}})$ and $r_{\mathrm{fs}} = (n_{\mathrm{f}}-n_{\mathrm{s}})/(n_{\mathrm{f}}+n_{\mathrm{s}})$ being the Fresnel reflection coefficients at the air-film ($r_{0\mathrm{f}}$) and film-substrate (r_{fs}) interface. Here $n_{\mathrm{f}} = (i\sigma^*/\varepsilon_0\omega^*)^{1/2}$ and n_{s} are the complex refractive indices of the film and substrate, respectively, λ is the radiation wavelength, d is the film thickness, $\omega = 2\pi\nu$ is the angular frequency, $\sigma^* = \sigma_1 + i\sigma_2$ is the complex conductivity of the film, and ε_0 is the permittivity of free space. Equation (1) is written neglecting the multiple reflections from the opposite sides of the substrate.

The experimentally obtained reflectance $R = |r|^2$ does not provide enough information to calculate the film conductivity above $40\,\mathrm{cm}^{-1}$ because of the unknown phase shift. Therefore, a Kramers-Kronig analysis has to be applied to the reflectance data. The condition of the applicability of this kind of analysis to the substrate-film system is the analyticity of $\log|r|$ in the upper half-plane [21]. The absence of the poles in $\log|r|$ is ensured by the relation $|r| \leq 1$. The absence of zeros in $|r|$ (*i.e.* branch points in $\log|r|$) follows from the analysis of the numerator of eq. (1): the term $r_{0\mathrm{f}}$ gives the reflectivity of the metal-vacuum boundary and therefore is close to (-1), the term $r_{\mathrm{fs}} \exp[4\pi i n_{\mathrm{f}} d/\lambda]$ is suppressed due to the presence of the exponent.

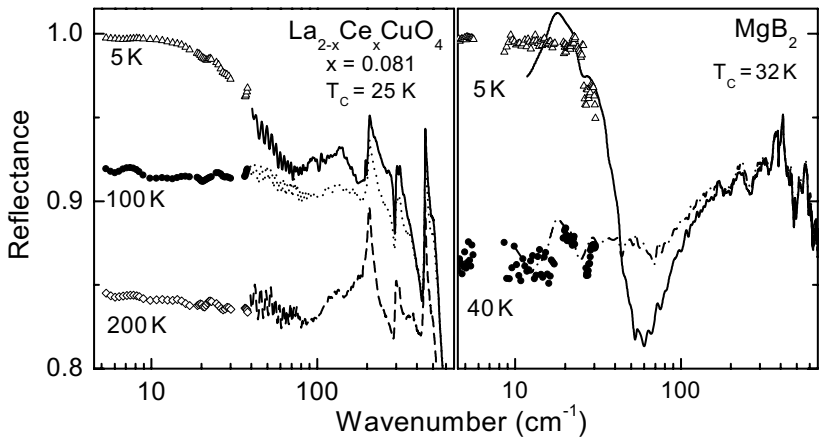

Fig. 1 – Far-infrared reflectance of an underdoped LCCO film at different temperatures (left panel). Lines: directly measured data; symbols: reflectance as calculated from the complex conductivity measured by submillimeter transmission technique. The right panel shows the reflectance of the MgB_2 film [14, 16] for comparison.

If the film thickness is smaller than the penetration depth ($|n_\mathrm{f}|d \ll \lambda$) and if $|n_\mathrm{f}| \gg |n_\mathrm{s}|$, eq. (1) can be simplified to

$$r \approx \frac{1 - \sigma^* dZ_0 - n_\mathrm{s}}{1 + \sigma^* dZ_0 + n_\mathrm{s}}\,, \tag{2}$$

where $Z_0 = \sqrt{\mu_0/\varepsilon_0} \simeq 377\,\Omega$ is the impedance of free space. Equation (2) provides a good approximation of the reflectance at submillimeter frequencies. For higher frequencies, eq. (1) has to be used. From eq. (2) the influence of the substrate properties on the conductivity spectra can be estimated. Except for the region close to phonons of the substrate, the refractive index of $SrLaAlO_4$ is $|n_\mathrm{s}| \leq 4$ and the term corresponding to the LCCO film can be estimated as $|\sigma^* dZ_0| \sim 50$. Therefore, the substrate contributes only about 10% of the total reflectance, and this contribution is further reduced using eq. (1). The presented procedure has been verified using model calculations, which completely reproduced the film conductivity without the effect of the substrate. The experimental uncertainties of real experiment lead to residual influence of the substrate on the film conductivity, which is especially important close to sharp phonon structures of $SrLaAlO_4$.

Results and discussion. – The left panel of fig. 1 shows the far-infrared reflectance of the underdoped LCCO film at different temperatures. At low frequencies and in the normally conducting state, the reflectance is approximately frequency independent. This behavior is strongly different from the well-known asymptotic law for a bulk metal in the Hagen-Rubens limit ($1 - R \propto \sqrt{\nu}$). The observed frequency behavior is characteristic for a thin metallic film and is in agreement with eq. (2) for a metal at low frequencies with $\sigma^* \simeq \sigma_1$. A common feature of all spectra at higher frequencies is a sharp structure above $200\,\mathrm{cm}^{-1}$ which is due to the phonons of the substrate. The influence of the substrate is reduced substantially by calculating the complex conductivity via eq. (1) but cannot be fully removed.

In the superconducting state the low-frequency reflectance of the LCCO film becomes frequency dependent and follows approximately $1 - R \propto \nu^2$. Comparing the reflectance of LCCO in the superconducting state (fig. 1) with the spectra of an *s*-wave superconductor with comparable transition temperature, *e.g.* with the reflectance spectra of MgB_2 (right

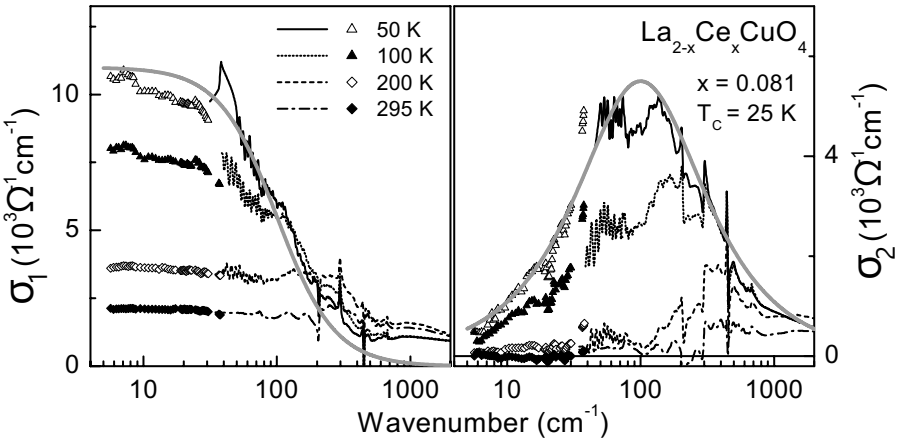

Fig. 2 – Far-infrared complex conductivity of an underdoped LCCO film above T_c. Left panel: σ_1, right panel: σ_2. The lines represent the conductivity obtained from the infrared reflectance, the symbols stand for the conductivity as measured directly by the submillimeter transmission technique. The thick gray line shows the prediction of the Drude model with $1/2\pi\tau = 100\,\mathrm{cm}^{-1}$.

panel) [14, 16], significant differences can be observed. In the spectra of MgB_2 the s-wave symmetry of the superconducting order parameter leads to a sharp "knee" in the reflectance around $h\nu \simeq 24\,\mathrm{cm}^{-1} \simeq 2\Delta_0$, which is in contrast to the spectra of LCCO where only a gradual decrease is observed. Thus, already the analysis of the reflectance spectra reveals a first indication of an unconventional gap-symmetry in LCCO.

Figure 2 shows the far-infrared conductivity of the underdoped LCCO film in the normally conducting state. The results above $40\,\mathrm{cm}^{-1}$ were obtained by applying the Kramers-Kronig analysis to the reflectance data and solving eq. (1). Below $40\,\mathrm{cm}^{-1}$ the complex conductivity was calculated directly from the transmittance and phase shift. We recall that the resonance-like structures between 200 and $700\,\mathrm{cm}^{-1}$ are due to the residual influence of the substrate. In this frequency range only the overall frequency dependence of the conductivity is significant. The far-infrared conductivity in the normally conducting state can well be described by the Drude model with a frequency-independent scattering rate $1/\tau$. At low frequencies, σ_1 is frequency independent and σ_2 increases approximately linearly with frequency. For frequencies close to the value of the scattering rate, σ_1 starts to decrease and σ_2 shows a maximum, $\nu_{\max} \simeq 1/2\pi\tau$. The gray solid line in fig. 2 provides a good description of the conductivity at $T = 50\,\mathrm{K}$ and demonstrates the validity of the Drude model for LCCO. Substantial deviations between the data and the model can be observed above $200\,\mathrm{cm}^{-1}$. These deviations can be described assuming a frequency dependence of the quasiparticle scattering, which agrees well with the infrared experiments in $(NdCe)_2CuO_4$ [22].

As has been proposed recently [23], a small ($\sim 1^\circ$) tilt of the sample surface from the ideal c-axis orientation leads to a conductivity peak at finite frequencies. In the present experiment, care has been taken to avoid such tilt effects, resulting in a peak-free real part of the infrared conductivity in the normal state.

The infrared conductivity changes dramatically upon entering the superconducting state. These data are represented in fig. 3. The real part of the conductivity is strongly suppressed below $100\,\mathrm{cm}^{-1}$ (left panel). Contrary to the conductivity of s-wave superconductors [16, 24], no clear onset of $\sigma_1(\nu)$ can be seen in the far-infrared range, which again indicates an un-

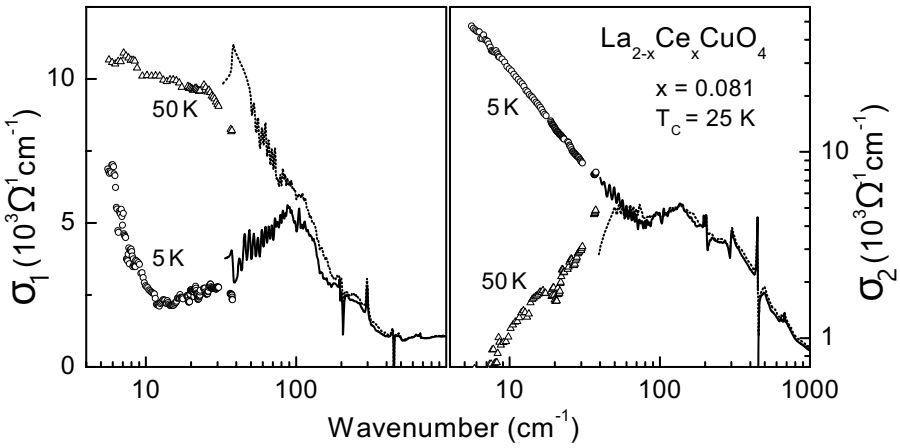

Fig. 3 – Far-infrared complex conductivity of an underdoped LCCO film above and below $T_c = 25\,\mathrm{K}$. The lines represent the conductivity obtained from the infrared reflectance, the symbols stand for the conductivity as measured directly by the submillimeter transmission technique.

conventional character of the energy gap. Instead, $\sigma_1(\nu)$ clearly reveals two contributions, a Drude-like quasiparticle peak at zero frequency and a finite-frequency peak close to $100\,\mathrm{cm}^{-1}$. A similar maximum at correspondingly higher frequencies has been observed in infrared experiments on hole-doped cuprates [25]. Assuming a spin fluctuation scenario of superconductivity, the frequency of the conductivity peak can be ascribed to the quadrupled frequency of the superconducting gap $4\Delta_0$ [26]. Compared to an s-wave superconductor with the conductivity onset at $2\Delta_0$, an additional shift by $2\Delta_0$ arises due to a four-particle final state. As has been shown recently, the residual attraction in a d-wave superconductor binds a particle and a hole into a spin exciton at an energy $\Delta_{\mathrm{spin}} < 2\Delta_0$ [27]. As a result, the optical conductivity reveals another characteristic feature at a frequency $2\Delta_0 + \Delta_{\mathrm{spin}}$. These mechanisms possibly explain the origin of the conductivity peak shown in fig. 3. Although the optical spectroscopy is not sensitive to a sign change of the superconducting order parameter, the conductivity data in fig. 3 provide strong experimental evidence for a highly anisotropic (and, possibly, d-wave) energy gap in underdoped LCCO: according to d-wave model calculations including spin fluctuation scattering, a gap with nodes gives rise to a residual Drude-like peak at $\omega = 0$ [28], and a maximum at finite frequencies resulting from inelastic-scattering processes [26, 27].

Due to the suppression of the conductivity at far-infrared frequencies, substantial spectral weight is removed from this frequency range and is transferred to the delta-function at zero frequency (superconducting condensate). This transfer leads to the dramatic increase of $\sigma_2(\nu)$ at low frequencies, $\sigma_2(\nu) \propto 1/\omega$, which corresponds to a zero-frequency penetration depth $\lambda_0 = 0.38 \pm 0.03\mu$. This value is in a good agreement with the data obtained by the low-frequency mutual inductance technique on similar samples [8].

At frequencies below $10\,\mathrm{cm}^{-1}$ and in the superconducting state, σ_1 shows a wing of the low-frequency excitations (left panel of fig. 3) which probably corresponds to a Drude-like quasiparticle peak [26,28]. The rate of the quasiparticle scattering is strongly suppressed compared to the normal state ($1/2\pi\tau \simeq 100\,\mathrm{cm}^{-1}$ at $T = 50\,\mathrm{K}$) and attains values around $10\,\mathrm{cm}^{-1}$.

Figure 4 shows the temperature dependence of the quasiparticle scattering of LCCO. The effective scattering rate has been obtained solely from the submillimeter-wave conductivity

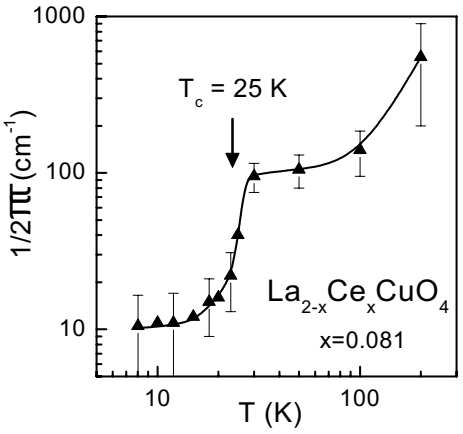

Fig. 4 – Temperature dependence of the effective quasiparticle scattering in LCCO. The data have been obtained from the two-fluid analysis of the submillimeter-wave conductivity, eq. (3).

($5\,\mathrm{cm}^{-1} < \nu < 40\,\mathrm{cm}^{-1}$) using a two-fluid analysis [17]:

$$\sigma^*(\omega) = \frac{\varepsilon_0 \omega_\mathrm{p}^2 \tau}{1 - i\omega\tau} + A\left[\frac{\pi}{2}\delta(0) + \frac{i}{\omega}\right]. \tag{3}$$

Here ω_p^2, τ, and A represent the plasma frequency, the scattering rate of quasiparticles, and the spectral weight of the superconducting condensate, respectively. In this equation, the delta-function $\delta(0)$ obviously does not influence the calculations at finite frequencies and the parameter A is obtained as low-frequency limit of $\sigma_2 \cdot \omega$.

The most prominent feature of fig. 4 is the suppression of the effective scattering rate directly at T_c. This is similar to the temperature dependence of the scattering rate in optimally doped $YBa_2Cu_3O_{7-\delta}$, where a drop in $1/\tau$ has been observed, *e.g.* using microwave resonator technique [29] or submillimeter transmission spectroscopy [17]. However, in case of $YBa_2Cu_3O_{7-\delta}$, the scattering rate revealed a linear temperature dependence above T_c, in contrast to LCCO where the scattering rate levels off for temperatures below $\sim 100\,\mathrm{K}$.

Conclusions. – In conclusion, combining two experimental techniques we obtained the far-infrared conductivity of underdoped $La_{2-x}Ce_xCuO_4$ in the frequency range above and below the gap frequency. No characteristic onset of absorption is observed in the superconducting state, which is inconsistent with the conventional BCS scenario. At low temperatures a maximum of infrared conductivity is observed at frequencies close to $100\,\mathrm{cm}^{-1}$ which is qualitatively similar to the properties of the hole-doped cuprates. The quasiparticle scattering rate is suppressed upon entering the superconducting state. These results provide experimental evidence for a *d*-wave or highly anisotropic *s*-wave gap in underdoped LCCO.

The stimulating discussion with P. J. Hirschfeld is gratefully acknowledged. This work was supported by BMBF (13N6917/0 - EKM).

REFERENCES

[1] Tokura Y., Takagi H. and Uchida S., *Nature*, **337** (1989) 345.
[2] Wu D.-H. *et al.*, *Phys. Rev. Lett.*, **70** (1993) 85; Andreone A. *et al.*, *Phys. Rev. B*, **49** (1994) 6392; Schneider C. W. *et al.*, *Physica C*, **233** (1994) 77.
[3] Stadlober B. *et al.*, *Phys. Rev. Lett.*, **74** (1995) 4911.
[4] Alff L. *et al.*, *Phys. Rev. Lett.*, **83** (1999) 2644.
[5] Tsuei C. C. and Kirtley J. R., *Rev. Mod. Phys.*, **72** (2000) 969.
[6] Prozorov R. *et al.*, *Phys. Rev. Lett.*, **85** (2000) 3700; Kokales J. D. *et al.*, *Phys. Rev. Lett.*, **85** (2000) 3696.
[7] Sato T. *et al.*, *Science*, **291** (2001) 1517; Armitage N. P. *et al.*, *Phys. Rev. Lett.*, **86** (2001) 1126.
[8] Skinta J. A. *et al.*, *Phys. Rev. Lett.*, **88** (2002) 207005.
[9] Biswas A. *et al.*, *Phys. Rev. Lett.*, **88** (2002) 207004.
[10] Naito M., Karimoto S. and Tsukada A., *Supercond. Sci. Technol.*, **15** (2002) 1663.
[11] Fournier P., Maiser E. and Greene R. L., *Gap Symmetry and Fluctuations in High-T_c Superconductors*, edited by Bok J. *et al.* (Plenum Press, New York) 1998, p. 145.
[12] Nagamatsu J. *et al.*, *Nature*, **410** (2001) 63.
[13] Posazhennikova A. I., Dahm T. and Maki K., *Europhys. Lett.*, **60** (2002) 134.
[14] Pimenov A., *Adv. Solid State Phys.*, **42** (2002) 267.
[15] Pronin A. V. *et al.*, *Phys. Rev. B*, **57** (1998) 14416.
[16] Pimenov A., Loidl A. and Krasnosvobodtsev S. I., *Phys. Rev. B*, **65** (2002) 172502.
[17] Pimenov A. *et al.*, *Phys. Rev. B*, **61** (2000) 7039.
[18] Naito M. and Hepp M., *Physica C*, **357-360** (2001) 333; *Jpn. J. Appl. Phys.*, **39** (2000) L485.
[19] Kozlov G. V. and Volkov A. A., *Millimeter and Submillimeter Wave Spectroscopy of Solids*, edited by Grüner G. (Springer, Berlin) 1998, p. 51.
[20] Heavens O. S., *Optical Properties of Thin Solid Films* (Dover Publications, New York) 1991.
[21] Cardona M., *Optical Properties of Solids*, edited by Nudelman S. and Mitra S. S. (Plenum Press, New York) 1969, p. 137.
[22] Homes C. C. *et al.*, *Phys. Rev. B*, **56** (1997) 5525; Singley E. J. *et al.*, *Phys. Rev. B*, **64** (2001) 224503.
[23] Pimenov A. *et al.*, *Phys. Rev. B*, **66** (2002) 212508.
[24] Palmer L. H. and Tinkham M., *Phys. Rev.*, **165** (1968) 588.
[25] Schützmann J. *et al.*, *Europhys. Lett.*, **8** (1989) 679; Basov D. N. *et al.*, *Phys. Rev. Lett.*, **74** (1995) 598.
[26] Quinlan S. M., Hirschfeld P. J. and Scalapino D. J., *Phys. Rev. B*, **53** (1996) 8575.
[27] Abanov A., Chubukov A. V. and Schmalian J., *Phys. Rev. B*, **63** (2001) 180510R.
[28] Hirschfeld P. J., Putikka W. O. and Scalapino D. J., *Phys. Rev. Lett.*, **71** (1993) 3705; *Phys. Rev. B*, **50** (1994) 10250.
[29] Bonn D. A. and Hardy W. N., *Physical Properties of High Temperature Superconductors*, edited by Ginsberg D. M., Vol. **V** (World Scientific, Singapore) 1996, p. 7.